

Geospatial technique based flood hazard assessment and mapping: a case study of Orang National Park, Assam, India

Rani Kumari Shah¹ and Rajesh Kumar Shah²

¹*Department of Geography, Cotton University, Guwahati, Assam, India*

²*Department of Zoology, D.H.S.K.College, Dibrugarh, Assam, India*

6.1 Introduction

Natural disasters are the result of various geological, hydrological, as well as meteorological events that lead to significant loss of life, property, and damage to the natural landscapes. As estimated by the United Nations office for Disaster Risk Reduction, these natural hazards claim nearly 42 million lives annually on a global scale and result in an average economic loss of 293 billion USD (UNDRR, 2017). Flood is the most frequently occurring hydrometeorological hazards with a profound impact (Gupta & Dixit, 2022). A severe hike in the frequency and severity of flood events has been witnessed in recent years due to various factors such as irregular rainfall (RF) patterns, river overflows, rapid melting of snow, deforestation, unregulated urbanization and unorganized human settlements along the riverbanks and coastal regions, and so forth (Armenakis, Du, Natesan, Persad, & Zhang, 2017). Flood is among the world's most devastating disasters that cause more casualties and damage to property than any other natural phenomenon (Duan et al., 2014; Forkuo, 2011; Hapuarachchi, Wang, & Pagano, 2011; Tsakiris, 2014; Wang, Li, Tang, & Zeng, 2011). Apart from its severe impact on humans and the environment, it is also one of the most complex phenomenon to model and prepare for. Extreme RF, failures of dams, tsunamis, and storm surges are some of the potential drivers that increase its complexities (Glas et al., 2019; Zwenzner & Voigt, 2009; UNDRR, 2019). Thus it is very important to recognize flood as a potential threat due to their potential for extensive destruction (Stefanidis & Stathis, 2013).

India is the second most flood-prone country in the world, next to China. It encounters around 17 flood events annually on average, affecting nearly 345 million individuals (CRED, 2020). The extensive river network found in India and

the monsoon system exacerbate its vulnerability, resulting in the flooding of around 5.74 million hectares of its total land surface (Dhar & Nandargi, 2004; Subrahmanyam, 1988). Assam is a north eastern state of India that faces significant flood risks due to the complex and braided nature of the river Brahmaputra. The periodic floods in this region occur every year and cause havoc and are a major concern in Assam. These floods are caused by heavy RF due to monsoon and snow melt from the Himalayas. Other factors like erosion and human settlements along the flood-prone regions contribute to the severity of flooding. Orang National Park (ONP) is situated within the floodplain of the river Brahmaputra. Brahmaputra flows along the southern boundary of the park and forms a complex network of channels, especially during the monsoon season. Small tributaries like Pachnoi and Dhansiri flow along the park's boundaries, eventually joining the Brahmaputra River. The dynamic channels form several *beels* all over the area. Close proximity of the park to the river as well as its low terrain render it highly susceptible to flooding, mostly during the monsoon season (Hazarika & Saikia, 2010). The park is a home to diverse plants and animals that include many rare and threatened species. Some of the important fauna found here are One-horned *Rhinoceros*, Asiatic elephant, Royal Bengal tiger, Indian hog deer, wild buffalo, pygmy hog, Gangetic dolphin, Indian pangolin, hog deer, *Rhesus macaque*, porcupine, Indian fox, small Indian civet, otter, leopard cat, jungle cat, tortoise, turtle, pythons, and cobras. More than 280 species of birds have been recorded in the park by several workers (Chakdar, Singha, & Choudhury, 2019; Choudhury, 2000; Rahmani, Narayan, Rosalind, & Sankaran, 1990). Some important bird species include Bengal florican, Baer's pochard, Greater adjutant, vultures, yellow-throated sparrow, brown-headed barbet, bristled grass-warbler, black-necked stork, greater adjutant stork, spot-billed pelican, great white pelican, Bengal florican, and lesser adjutant. Some important flora of the park include *Saccharum spontaneum*, *Imperata cylindrica*, *Apluda mutica*, *Dysoxylum binectariferum*, *Melia azadirachta*, *Sterculia villosa*, and *Toona ciliate* (Chakdar et al., 2019). The frequent flooding event in Assam causes profound impacts on both humans and wildlife (Debbarma & Deen, 2020). A significant portion of the ONP was inundated during the flood event that took place in 2022, causing substantial damage, and several antipoaching camps were submerged under water.

Due to severe flood events occurring all over the world and the severe damages they cause, flood hazard mapping has become very important. The major objective of flood hazard mapping is to effectively manage floods that result from factors like heavy RF, dam overflows, and so forth, which aims to minimize the adverse impacts on lives and property. The development of a flood hazard map is very useful in assessing and mitigating flood-related risks in vulnerable areas (Zhang, Zhou, Xu, & Watanabe, 2002). Flood hazard mapping is one of the most significant approaches that is used to evaluate the risk of flooding in a particular area. Such an approach utilizes a combination of qualitative and semiquantitative methods considering a wide range of environmental factors such as the shape of

the land, soil type, the amount of precipitation, land use in the area, and the hydrological properties of the surrounding watersheds (Hallegatte, Green, Nicholls, & Corfee-Morlot, 2013). Such an assessment is essential because it helps us to predict flood hazard that is important for developing effective strategies to manage floods and to promote sustainable environmental practices. One of the key aspects of assessment of flood hazard is the generation of flood hazard maps that can play an important role in land use planning in flood-prone regions and also help in identifying areas at high risk of flooding (Khaing et al., 2019). Such maps are user-friendly and easily used by the planners to pinpoint areas that need immediate attention and prioritize flood mitigation efforts (Ajin, 2013; Bapalu & Sinha, 2005; Danumah et al., 2016; Forkuo, 2011; Wang et al., 2011; Argaz, 2019). Flood hazard mapping and analysis is also an important part of early warning systems for preventing and mitigating future food situations. Some of the commonly used models for flood hazard mapping include the analytical hierarchy process (AHP), frequency ratio model, artificial neural networks, hydrological simulation program-FORTRAN, hydrological forecasting systems, HEC-RAS, storm water management model, logistic regression, generalized linear models, entropy, k-nearest neighbors, random forest, weight of evidence, Shannon's entropy model, gray decision-making trial and evaluation laboratory, support vector machine, erosion models, and kinematic runoff (Bhatt, Sinha, Deka, & Kumar, 2014; Shah & Shah, 2023a,b; Wiles & Levine, 2002; FLAouacheria, Kechida, & Chabi, 2019; Fonseca, Santos, & Santos, 2018; Rangari, Sridhar, Umamahesh, & Patel, 2019; Youssef, Pradhan, & Sefry, 2016; Rahmati et al., 2019). Use of remote sensing (RS) and geographic information system (GIS) software tools has gained popularity in recent years due to their ability to provide essential justification and fresh perspective for vulnerability assessments. These tools provide significant insights into specific areas, specifically when satellite imagery is analyzed. The integration of RS and GIS for flood hazard assessment is currently prevalent and highly effective and provides highly accurate maps (Ali, Khatun, Ahmad, & Ahmad, 2019). They serve as an important tool for devising flood hazard risk assessment strategies through the multicriteria analysis (MCA) approach (Arya & Singh, 2021; El-Haddad et al., 2021). The MCA approach is found to be multifunctional and valuable by several workers (Antoine, Fischer, & Makowski, 1997; Rikalovic, Cosic, & Lazarevic, 2014; Gil & Kellerman, 1993; Pohekar & Ramachandran, 2004; Saki, Dehghani, Jodeiri Shokri, & Bogdanovic, 2020; Saleh, Aliani, & Amoushahi, 2020; Wang, Jing, Zhang, & Zhao, 2009). The advanced software tools can simplify the process of preparing flood hazard maps that can give valuable results for mapping flood susceptibility and vulnerability. Such maps are widely acceptable and considered to be more credible.

Very limited reports on the flooding events and their impacts are available as far as ONP is concerned. Given these circumstances, there is an urgent need to undertake a comprehensive study on flood risk assessment in order to identify

vulnerable areas and contributing factors. Thus the flood hazard mapping of ONP becomes vital in order to minimize and prevent the potential damage to the park and wildlife in future. As ONP is a homeland for various plants and animals including several globally threatened fauna, any damage to their habitat may also lead to their extinction in the future. Thus our present study on flood hazard mapping of ONP is very crucial. The main objective of this study is to develop a flood hazard map for the ONP utilizing RS and GIS techniques, with the application of the AHP model. By identifying various flood controlling factors within the study area and employing AHP modeling, the aim is to provide a valuable tool for policymakers and planners to mitigate flood hazards in this globally important park effectively. The present study is the first attempt to categorize the study area in different flood susceptible zones using AHP integrated with RS-GIS. No study on flood susceptibility has been carried out earlier in this rich national park.

6.2 Materials and methods

6.2.1 Description of the study area

ONP is situated in Darrang and Sonitpur districts of Assam and is very popular for its diverse flora, fauna, and esthetic beauty. The geographical extension of the park is between 26°28'49.0891"N to 26°35'43.6644"N latitude and 92°14'50.1272"E to 92°24'56.1071"E longitude. It is often known as “mini Kaziranga” due to its landscape being similar to the Kaziranga National Park and its rich population of one-horned *Rhinoceros*. The park is surrounded by the river Brahmaputra on the south, its tributary Dhansiri on the west, and Panchnoi on the east. The northern part of the park is bounded by Nalbari and villages of Darrang district. Due to the close proximity of the park to these three rivers, Orang forms a vital part of the Indo-Burma biodiversity hotspot and is among the attractive parks of Assam that covers an area of 78.08 km². The terrain of the region is flat that shows general slopping from north to south. The altitude ranges between 48 and 90 m above the mean sea level. Both young and old alluvial soil are found with varying humus contents and the texture varies from sandy loam to silty loam in nature (Talukdar & Sharma, 1995). The park experiences an average annual RF of 1910 mm (Sarma, Mipun, Talukdar, Kumar, & Basumatary, 2011). A map of the study area is shown in Fig. 6.1.

6.2.2 Sources of data

Various secondary data were used in the present study. These data sources include satellite imagery, digital elevation model (DEM), and climatic data (RF). The Landsat sentinel 2 A image taken on January 19, 2023, was downloaded from US Geological Survey (USGS) Earth Explorer (<https://earthexplorer.usgs.gov>) website

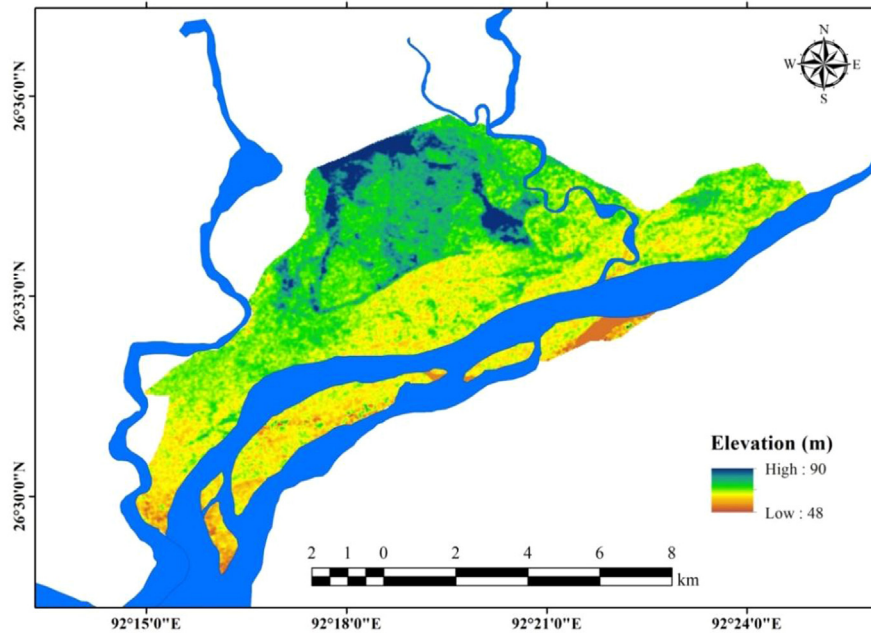


FIGURE 6.1

Study area map.

with 5% cloud cover, which offers satellite images with significant spatial and spectral resolution from different time intervals across the world. Landsat sentinel 2 A images have 10 m spatial resolution and are capable of monitoring the features of the earth's surface such as land use and cover, vegetation health, and drainage characteristics, all of which directly impact flood events in any region. The sentinel 2-A satellite image was georeferenced to the World Geodetic System 1984 datum and Universal Transverse Mercator Zone 46 N coordinate system. Additionally, SRTM DEM data with a 30 m spatial resolution was accessed through the USGS Earth Explorer (<https://earthexplorer.usgs.gov>). DEM data provide detailed terrain information, and such data can significantly contribute to flood hazard mapping (Muhadi, Abdullah, Bejo, Mahadi, & Mijic, 2020). RF data ($0.25^{\circ} \times 0.25^{\circ}$ gridded datasets) were obtained from the India Meteorological Department for the year 2022 (Pai et al., 2014). Such high-resolution RF data are very essential for flood modeling and mapping.

6.2.3 Preparation of flood controlling factors

Based on the literature review, personal observation, and discussion with local residents, the flood controlling factors were determined. Accordingly, elevation

(E), slope (S), land use and land cover (LULC), proximity to river, drainage density (DD), normalized difference vegetation index (NDVI), topographic wetness index (TWI), RF, and flow accumulation (FA) were considered as important flood controlling factors in ONP. Table 6.1 depicts the details of mode of preparation of each factor.

6.2.4 The analytical hierarchy process model

The AHP, introduced by Saaty (1980), is a prominent decision-making approach using multiple criteria evaluation. It offers a structured approach to systematically compare and weigh different criteria by employing pairwise comparisons. Relative importance of one criterion over another can be easily accessed by the decision-makers, producing a pairwise comparison matrix (Malczewski, 2000). A standardized scale ranging from 1 to 9 is used in this method where 1 denotes equal importance, 3 moderate importance, 5 strong importance, 7 very strong importance, and 9 extreme importance. Its ability to facilitate group decision-making has been the main compelling aspect of its wide adoption, global recognition, and application. The AHP is a straightforward and adaptable method that is widely used in flood analysis, as it delivers precise outcomes. It can play a vital role in managing flood by helping decision-makers prioritize and make necessary choices regarding various strategies of flood hazard reduction, allocation of resources, and response planning. The model can be used to study various factors and the complex relationship between them in flood hazard assessment. For each controlling factors, the rank values were assigned on the basis of their relative importance on a scale from 1 to 9. Depending upon the importance of the flood-causing factors, pairwise and normalized pairwise comparison matrices were prepared. Weight values of each flood-causing factor were computed, and consistency ratio (CR) was calculated (Saaty & Vargas, 2000; Saaty, 1977, 1980, 1990, 2008). As nine flood-causing factors were considered in the present study, the value of random consistency index is taken as 1.45. The methodological flowchart is shown in Fig. 6.2.

$$\text{Consistency ratio (CR)} = \frac{\text{CI}}{\text{RI}}$$

where

$$\text{CI(consistency index)} = \frac{\lambda - n}{n - 1}$$

RI = random index (1.45 for nine factors)

n = number of flood-causing factors

λ = average value of the consistency vector

Table 6.1 Methods used in preparation of each factor.

Factors	Mode of preparation of each factor
E	E plays a critical role in influencing the occurrence of floods (Shah & Shah, 2023a,b). Generally areas at lower Es are more susceptible to flooding. The spatial E map was created using DEM data and was categorized into five classes in ArcGIS 10.8.2 software.
S	S is a crucial factor in understanding and predicting flood events. The S map was developed from SRTM DEM using the surface tool in ArcGIS 10.8.2 software and was classified into five groups.
PR	PR increases the susceptibility to flooding compared to areas located further away (Glenn et al., 2012). The PR map is prepared using the Euclidean distance tool in ArcGIS 10.8.2 software (Arora, Pandey, Siddiqui, Hong, & Mishra, 2021; Shadmehri Toosi, Calbimonte, Nouri, & Alaghmand, 2019).
DD	The amount of runoff within a basin is directly and markedly influenced by the river density. Regions characterized by higher river density are at a heightened risk of experiencing floods. The DD map was prepared using ArcGIS 10.8.2 software and was grouped into five classes using quantile classification tool.
LULC	LULC patterns have a profound influence on a region's hydrology and can significantly impact the frequency severity of flood The LULC classification was performed using supervised classification method (maximum likelihood algorithm). The map was classified into five classes such as moist deciduous forest, swampy land, water bodies, sandbars, and dry grassland.
NDVI	The NDVI is a vegetation health indicator which assesses the health of vegetation. It plays a crucial role in understanding floods dynamics. It ranges from -1 to +1 (Khosravi, Nohani, Maroufinia, & Pourghasemi, 2016). Here, NDVI values were calculated using Landsat sentinel 2 A image based on following formula $\text{NDVI} = (\text{NIR} - \text{VIS}) / (\text{NIR} + \text{VIS}),$ where NIR = near infrared band, VIS = visible band
RF	RF is one of the primary triggers of flooding. Seasonal RF patterns can lead to prolonged and widespread flooding in certain regions. Spatial map of RF pattern was developed using interpolated method by the inverse distance weighting tool in ArcGIS 10.8.2 (Shadmehri Toosi et al., 2019).
TWI	TWI quantifies the prosperity of an area to accumulate water. A higher TWI value indicates areas with a greater to retain water, making them more vulnerable to flooding. Here, S and DEM data were applied to compute TWI using following formula $\text{TWI} = \ln(F) / (10 S)$
FA	FA is essential for predicting flood hazard. Areas with high FA are more likely to experience flood (Vojtek & Vojteková, 2019). FA raster map was prepared by DEM data using the hydrology tool in ArcGIS 10.8.2 software.

DD, Drainage density; DEM, digital elevation model; E, elevation; FA, flow accumulation; LULC, land use and land cover; NDVI, normalized difference vegetation index; PR, proximity to river; RF, rainfall; S, slope; TWI, topographic wetness index.

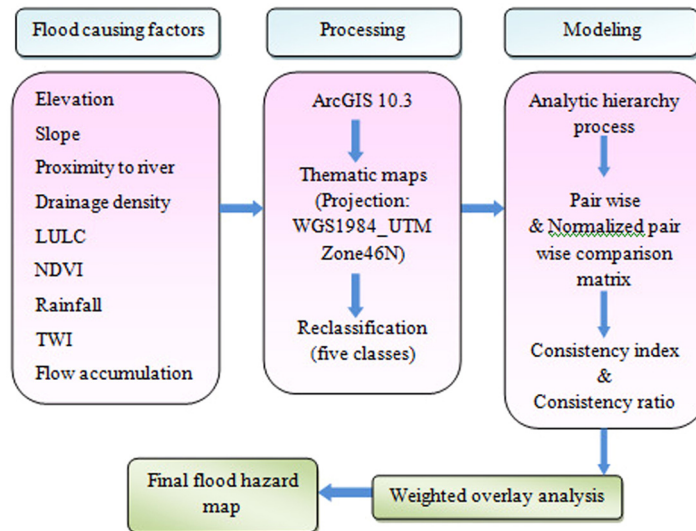


FIGURE 6.2

Methodological flowchart.

6.3 Results

Our research focused on identifying and examining nine flood-causing factors employing rigorous statistical methods for a comprehensive assessment. All the nine factors were subdivided into five classes, as shown in Table 6.2.

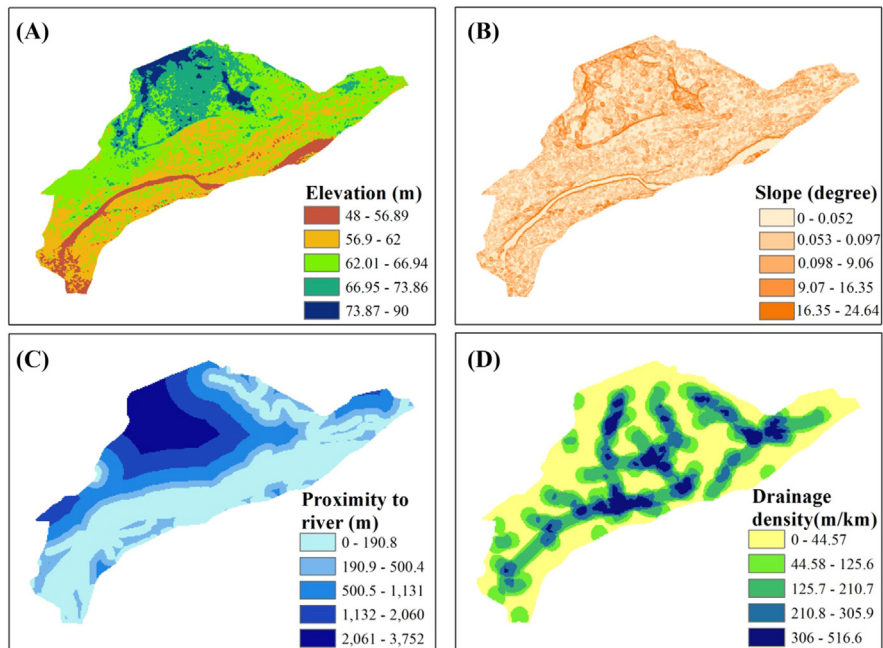
Thematic maps were prepared for all the factors and were classified in five different classes showing their spatial distribution. One of the most crucial factors causing flooding in a particular area is the elevation of that region. Generally, water flows from a higher elevation toward a lower elevation. Floods tend to be common on flat terrains with smaller altitude values due to their inverse relationship with the probability of occurrence and thus serve as an accurate indication of vulnerability due to floods (Hammami et al., 2019). The park ranges from 48 to 90 m in elevation. Low elevated regions such as water bodies adjacent to others are covered with water. The red represents the highest elevation from a western perspective of the park, while the dark blue demonstrates the lowest elevation toward the south-eastern end of the park (Fig. 6.3A).

The aspect of the slope is essential in indicating surface zonation, and the rate and duration of the water flow largely depend on the slope. The water moves slower, piles up for a longer time, and accumulates longer on a flatter surface, leading to flood (Rimba, Setiawati, Sambah, & Miura, 2017). The slope of the study area was from 0° to 24.64° . The areas with the slope within 0° – 0.052° and 0.053° – 0.097° indicates water bodies and flat lands with a very gentle slope,

Table 6.2 Classes of flood-causing factors and weight.

Factor	Class	Hazard class rating	Weight (%)
Elevation (m)	48–56.89	5	13
	56.9–62	4	
	62.01–66.94	3	
	66.95–73.86	2	
	73.87–90	1	
Slope (degree)	0–0.052	5	11
	0.053–0.097	4	
	0.098–9.06	3	
	9.07–16.35	2	
	16.35–24.64	1	
Proximity to river (m)	0–190.8	5	19
	190.9–500.4	4	
	500.5–1131	3	
	1132–2060	2	
	2061–3752	1	
Drainage density (m/km)	0–44.57	1	13
	44.58–125.6	2	
	125.7–210.7	3	
	210.8–305.9	4	
	306–516.6	5	
LULC (level)	Moist deciduous forest	1	12
	Water bodies	5	
	Swampy land	3	
	Sandbars	4	
	Dry grassland	2	
NDVI (level)	–0.145 to 0.0267	5	7
	0.0268–0.161	4	
	0.162–0.266	3	
	0.267–0.368	2	
	0.369–0.54	1	
Rainfall deviation (mm/year)	1770–1839	3	8
	1840–1894	2	
	1895–1941	1	
	1942–1998	1	
	1999–2111	2	
TWI (level)	–16.52 to –7	1	8
	–6.999 to –3.417	2	
	–3.416 to –0.1418	3	
	–0.1417 to 2.724	4	
	2.725–9.583	5	
Flow accumulation	0–2.056.8	1	10
	2056.9–8432.8	2	
	8432.9–18,511	3	
	18,512–28,795	4	
	28,796–52,448	5	

LULC, *Land use and land cover*; NDVI, *normalized difference vegetation index*; TWI, *topographic wetness index*.

**FIGURE 6.3**

Flood-causing factors: (A) elevation, (B) slope, (C) proximity to river, and (D) drainage density.

which are suitable for occurrence of floods compared to areas with a moderate to steep slope (Fig. 6.3B). Flood inundation is more intense in areas closer to a stream confluence compared to those remote, since at a point of a stream confluence, the channel often carries a combined load and flow of two or more upstream tributaries. When a river overflows, the flow is more than the drainage capacity of the river, and therefore, it increases the depth of the water around river margins. This flood will not affect only the closest river point, but the surrounding areas will also experience water flooding and risks of flood (Chakraborty & Mukhopadhyay, 2019). Classification of the study area was done into five classes ranging from 0 to 190.8, 190.9 to 500.4, 500.5 to 1131, 1132 to 2060, and 2061 to 3752 m. The areas grouped as very high and high flood risk are located within 0–190.8 and 190.9–500.4 m, respectively, as depicted in Fig. 6.3C. Additionally, DD is another major element that significantly adds to the flood occurrence in a place (Onuşluel Gül, 2013). DD per unit area has a direct impact on runoff occurring from the basin. Areas of a high river concentration are susceptible to flooding (Shah & Shah, 2023a,b). This analysis revealed that the minimum DD was between 0 and 44.57 m/km, while the maximum was a high of 516.6 m/km, as shown in Fig. 6.3D. Flood susceptibility is higher in an

area with high DD than in an area with a low DD. The impact of various LULC types on susceptibility to flooding in any region can be quite substantial. The interrelationship of various hydrological parameters such as runoff, infiltration, and RF abstraction is controlled by the LULC. For example, forests and natural trees enhance water penetration and seepage. Significant parts covered by water, sand, and marshlands have an immense influence on flooding. The LULC classification of the park is categorized as moist deciduous forest (19.4 km²), swampy land (33.15 km²), water bodies (10.83 km²), sandbars (4.20 km²), and dry grassland (10.5 km²). The dominant LULC in the study area is swamps (42.45%), as depicted in Fig. 6.4A.

The presence of vegetation across any surface also causes reduction in speed of flow of water while increasing soil water infiltration associated with that surface (Zhao et al., 2019). Vegetative cover is helpful in reducing the magnitude and swiftness of flood. A high positive value indicates high density, thus implying that the area is covered with dense forests, while a low positive value indicates low density, thus implying that the area has grasslands or shrubs. Flood susceptibility goes down as NDVI increases. NDVI varied between 0.145 and 0.54 for the study area. A spatial distribution map indicates high frequency of very low and

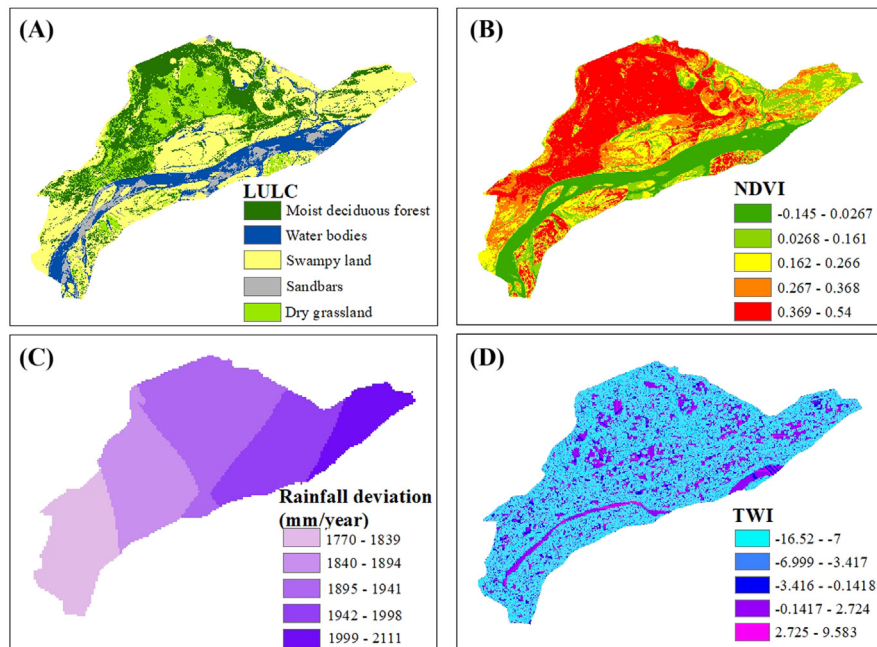


FIGURE 6.4

Flood-causing factors: (A) land use and land cover, (B) normalized difference vegetation index, (C) rainfall deviation, and (D) topographic wetness index.

low index zones within the southern, south-eastern, and southwestern regions portrayed as green and light green coloration, as shown in Fig. 6.4B. The probability of flood in an area increases with the increasing RF within a specific time period. The RF value was found to be in between 1770 and 2111 mm/year. RF deviation in the study area has been categorized into five classes: 1770–1839, 1840–1894, 1895–1941, 1942–1998, and 1999–2111 mm/year (Fig. 6.4C). The amount of soil moisture in an area can be forecast using TWI, which describes the tendency of accumulated water in that particular area. The TWI index clearly depicts how a slope affects hydrological processes. TWI explains the water accumulation trend at a particular region, and the local slope shows the influence of gravitational forces on the flow of water (Fernández & Lutz, 2010; Pourali, Arrowsmith, Chrisman, Matkan, & Mitchell, 2016). A spatial distribution map of TWI was prepared and grouped into five classes such as -16.52 to -7 , -6.999 to -3.417 , -3.416 to -0.1418 , -0.1417 to 2.724 , and 2.725 to 9.583 . The pink color depicted the highest values, which is shown in Fig. 6.4D. FA is also an essential parameter in determining flood hazards. The values of accumulated flow show regions with a concentrated water flow area, thereby indicating the probability of a flood hazard. The thematic map was grouped into five classes such as $0-2,056.8$, $2,056.9-8,432.8$, $8,432.9-18,511$, $18,512-28,795$, and $28,796-52,448$ (Fig. 6.5A). The higher score of FA indicates that the area has lower probability flood hazards because of its less concentrated water in that area and vice versa.

Table 6.3 presents the pairwise matrix, while Table 6.4 shows the normalized pairwise matrix of AHP. CR was computed and found to be 0.042 (Table 6.5). According to Saaty (1990), a CR value between 0 and 0.1 is considered to be consistent. Hence, in the present case, the CR value can be acceptable in decision-making. The CI value was found to be 0.061. The factors were prioritized in a systematic approach as per the geographical characteristics of the study area,

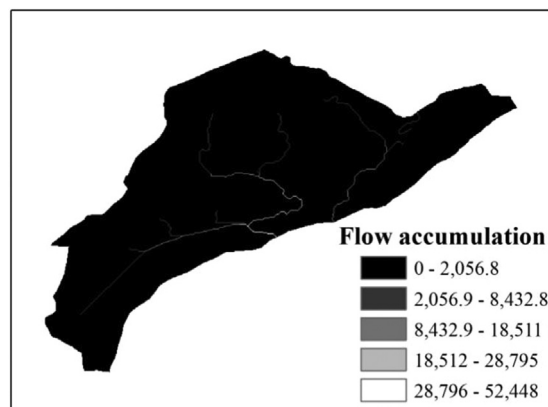


FIGURE 6.5

Flood-causing factors: flow accumulation.

Table 6.3 Pairwise comparison matrix.

Factors	E	S	PR	DD	LULC	NDVI	RF	TWI	FA
E	1	1	1	2	1	2	1	1	1
S	1	1	0.50	1	1	2	2	1	1
PR	1	2	1	2	2	3	2	3	2
DD	1	1	0.50	1	1	3	1	3	1
LULC	1	1	0.50	1	1	2	2	2	1
NDVI	1	0.50	0.33	0.30	0.50	1	1	1	1
RF	1	0.50	0.50	1	0.50	1	1	1	1
TWI	1	1	0.33	0.30	0.50	1	1	1	1
FA	1	1	0.50	1	1	1	1	1	1
Sum	9	9	5.16	9.60	8.50	16	12	14	10

DD, Drainage density; E, elevation; FA, flow accumulation; LULC, land use and land cover; NDVI, normalized difference vegetation index; PR, proximity to river; RF, rainfall; S, slope; TWI, topographic wetness index.

Table 6.4 Normalized pairwise comparison matrix.

Factors	E	S	PR	DD	LULC	NDVI	RF	TWI	FA
E	0.11	0.11	0.19	0.21	0.12	0.13	0.08	0.07	0.10
S	0.11	0.11	0.10	0.10	0.12	0.13	0.17	0.07	0.10
PR	0.11	0.22	0.19	0.21	0.24	0.19	0.17	0.21	0.20
DD	0.11	0.11	0.10	0.10	0.12	0.19	0.08	0.21	0.10
LULC	0.11	0.11	0.10	0.10	0.12	0.13	0.17	0.14	0.10
NDVI	0.11	0.06	0.06	0.03	0.06	0.06	0.08	0.07	0.10
RF	0.11	0.06	0.10	0.10	0.06	0.06	0.08	0.07	0.10
TWI	0.11	0.11	0.06	0.03	0.06	0.06	0.08	0.07	0.10
FA	0.11	0.11	0.10	0.10	0.12	0.06	0.08	0.07	0.10

DD, Drainage density; E, elevation; FA, flow accumulation; LULC, land use and land cover; NDVI, normalized difference vegetation index; PR, proximity to river; RF, rainfall; S, slope; TWI, topographic wetness index.

background information, and previous studies (Rahmati, Haghizadeh, & Stefanidis, 2016; Samanta, Bhunia, Shit, & Pourghasemi, 2018; Ullah and Zhang, 2020). The final weight for each factor is shown in Table 6.2.

A total of nine raster images (reclassified into 30 m spatial resolution) were used in the AHP model in order to identify the flood hazard zones. Flood hazard indices (FHIs) using the weight database were computed. The final thematic map of ONP was classified into four classes by weighted overlay tool in ArcGIS 10.8.2, namely, low (1–2), moderate (3), high (4), and very high (5) hazard

Table 6.5 Calculation of λ_{\max} , consistency index, and consistency ratio.

Factors	E	S	PR	DD	LULC	NDVI	RF	TWI	FA	Weighted sum value	Ratio
E	1.03	0.92	1.56	2.07	0.99	1.10	0.65	0.60	0.77	9.70	9.39
S	1.03	0.92	0.78	1.04	0.99	1.10	1.31	0.60	0.77	8.53	9.33
PR	1.03	1.83	1.56	2.07	1.97	1.65	1.31	1.81	1.54	14.78	9.47
DD	1.03	0.92	0.78	1.04	0.99	1.65	0.65	1.81	0.77	9.64	9.29
LULC	1.03	0.92	0.78	1.04	0.99	1.10	1.31	1.21	0.77	9.14	9.26
NDVI	1.03	0.46	0.52	0.31	0.49	0.55	0.65	0.60	0.77	5.39	9.81
RF	1.03	0.46	0.78	1.04	0.49	0.55	0.65	0.60	0.77	6.38	9.74
TWI	1.03	0.92	0.52	0.31	0.49	0.55	0.65	0.60	0.77	5.85	9.67
FA	1.03	0.92	0.78	1.04	0.99	0.55	0.65	0.60	0.77	7.33	9.53
Total											85.49
$\lambda_{\max} = 85.48/9$ = 9.498				CI = (9.49-9)/8 = 0.061				CR = 0.061/1.45 = 0.042			

CI, Consistency index; CR, consistency ratio; DD, drainage density; E, elevation; FA, flow accumulation; LULC, land use and land cover; NDVI, normalized difference vegetation index; PR, proximity to river; RF, rainfall; S, slope; TWI, topographic wetness index.

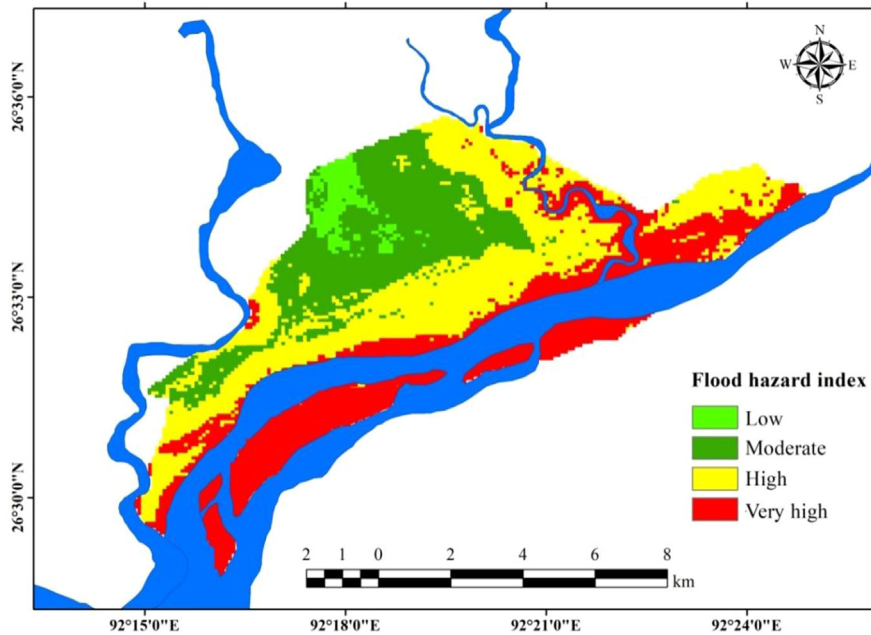


FIGURE 6.6
Flood hazard map.

Table 6.6 Statistics of flood hazard classes.

Sl. no.	Hazard class	Flood hazard indices	Area (%)
1	Low	1–2	4.14
2	Moderate	3	20.60
3	High	4	39.74
4	Very high	5	35.52

zones, as portrayed in Fig. 6.6 and Table 6.6. Higher FHI indicates high chances for flood events, while low FHI corresponds to scarce flood cases in this case.

Our study revealed that 35.52% of the land area of ONP falls under a very high hazard risk zone with an FHI of 5 and 39.74% under high and 20.60% under moderate hazard risk zone with FHI of 4 and 3, respectively. Only 4.14% of the total area is under low risk to flooding. By classifying the ONP into different hazard zones, our finding provides vital information, which will be crucial for management and planning purposes to mitigate the impacts of flooding on the park's ecosystem and wildlife. The study investigates various factors contributing

to flood risk, such as elevation, river density, slope gradient, forest cover, and the dynamic nature of river systems like the Brahmaputra and its tributaries. Understanding these factors can help in developing effective strategies for flood management and conservation efforts within the ONP. By linking flood risk to factors such as river dynamics and forest cover, our research may underscore the importance of conservation measures in mitigating the impacts of flooding on biodiversity and habitat loss.

6.4 Discussion

Flood hazard assessment forms part and parcel of flood management and mitigation that seeks to minimize the dangers associated with flooding. ONP located at the bank of Brahmaputra River has always been at risk of being submerged under water due to a series of occurrences of flooding throughout its existence. In cases of the flood hazard assessment, many parameters can be positive or negative depending on their properties in relation to the flood risk. Even though there is no general rule for deciding these factors, previous researchers have investigated different flood controlling elements considering the specificity of the site, data accessibility, and knowledge acquired from prior investigations (Rahmati et al., 2016; Samanta et al., 2018; Wang et al., 2011; Ullah & Zhang, 2020). As per our findings, more than 35% of the total area of the national park is under a high hazard risk zone. Very high and high hazard risk areas are mainly located along the adjoining parts of riverbanks. These areas fall toward the southern, south-eastern, and southwestern part of ONP. The high risk zone is found to have low elevation, higher river density, and slope gradient and is closely located to the active river channels. The low forest cover and the presence of large swamps along with the dynamic nature of river Brahmaputra and its tributaries (Dhansiri and Panchnoi) are mainly responsible for flooding in this area. The river Brahmaputra is also responsible for degradation of areas of Kaziranga and Dibru-Saikhowa national parks of Assam, as reported by Areendran et al. (2020) and Shah and Shah (2023a,b), respectively.

Being a national park, ONP is a habitat to thousands of plants and animals including some threatened and endemic organisms. The Royal Bengal tiger is the national animal of India, and more than 75% of world's tiger population is found in India. In 2016 the National Tiger Conservation Authority declares the park as a tiger reserve to boost the conservation of tigers in this region. The park is the 49th tiger reserve among 53 in India and one of the highly tiger-dense areas, which was reported to have a tiger population of 21 by Jhala and Qureshi (2019). According to the spatial distribution map of tiger prepared by the Assam forest department (Sandeep, 2020), some of the tigers are found in areas that according to our findings fall within high and moderate risk zones. The riverine islands which are very high risk to flood are also utilized by the tigers and other animals

such as elephants and ungulates from time to time, as reported by [Borah, Firoz, and Sarma \(2010\)](#). The findings highlight the critical importance of preserving the habitat within ONP for the conservation of its diverse and endangered wildlife, particularly the Royal Bengal tiger and the critically endangered Pygmy hog. With India hosting a significant portion of the world's tiger population, the designation of ONP as a tiger reserve in 2016 underscores its significance as a stronghold for tiger conservation efforts. The spatial risk zonation map developed in the study offers practical implications for wildlife conservationists, policymakers, and local authorities. By identifying high and moderate flood risk zones within the park, this map serves as a valuable tool for decision-making regarding habitat management and wildlife protection strategies. One practical implication is the need for targeted conservation measures to mitigate the impacts of flooding on wildlife populations, particularly those occupying high-risk zones. This may include the relocation of animals to less flood-prone areas during periods of heightened risk, thereby reducing the potential for habitat loss and population declines. Furthermore, the zonation map can inform land use planning and development policies within and around ONP. By delineating flood hazard risk zones, authorities can implement regulations to minimize human encroachment and infrastructure development in vulnerable areas, thereby reducing the potential for habitat fragmentation and degradation. The findings also underscore the importance of collaborative efforts among government agencies, nongovernmental organizations, and local communities in implementing effective conservation strategies. Community-based initiatives such as habitat restoration, antipoaching patrols, and public awareness campaigns can complement formal conservation measures and contribute to the long-term sustainability of ONP's biodiversity. Moreover, the study emphasizes the role of scientific research in informing evidence-based conservation practices. By conducting the first spatial risk zonation of ONP ([Fig. 6.6](#)), our research has provided valuable insights into the complex interactions between natural hazards and wildlife habitat suitability, laying the groundwork for future studies and conservation efforts in the region. The practical implications of the study findings extend beyond scientific research, offering actionable insights for wildlife conservation and land management practices in ONP. By leveraging the spatial risk zonation map, stakeholders can implement targeted conservation strategies to safeguard the park's rich biodiversity and ensure its long-term viability as a protected area.

6.5 Limitations of the study

1. One of the primary limitations of our study lies in the selection of flood-causing factors for the susceptibility analysis. While we considered nine factors based on available data, there is a lack of specific guidelines or standards for determining which factors to include. This limitation suggests

that our analysis may not encompass all relevant variables that could influence flood susceptibility. Consequently, there may be additional factors that were not accounted for in our model, potentially impacting the accuracy and comprehensiveness of our flood hazard map.

2. The AHP method utilized for assigning weights to the selected factors inherently involves a degree of subjectivity. The weights assigned to each factor depend on the knowledge and expertise of the researcher, as well as the availability and quality of data. This subjectivity introduces the possibility of error, as different researchers may prioritize factors differently or interpret their significance in varying ways. As a result, the accuracy of our flood hazard map may be influenced by the subjective decisions made during the weighting process, affecting the reliability of our results.
3. Another limitation stems from the reclassification of thematic maps, which can affect the resolution and accuracy of the final flood hazard map. The process of reclassifying data involves simplifying and categorizing information, which may lead to loss of detail or nuance. This loss of resolution could potentially obscure subtle variations in flood susceptibility within the study area, resulting in a less precise representation of flood risk. Therefore the reclassification process introduces a source of uncertainty that may compromise the reliability of our findings.
4. The lack of sufficient financial support represents a significant practical limitation of our study. Limited resources may have constrained our ability to collect comprehensive data, employ more sophisticated analytical techniques, or conduct field validations to enhance the robustness of our results. Additionally, financial constraints have hindered efforts to acquire specialized software or access additional datasets that could have enriched our analysis. Consequently, the scope and depth of our study may have been constrained by financial limitations, potentially impacting the thoroughness and accuracy of our findings.

While our study provides valuable insights into flood hazard mapping in the ONP, it is important to acknowledge these limitations, which may affect the comprehensiveness, accuracy, and reliability of our results. Future research efforts should aim to address these limitations by adopting more systematic approaches to factor selection, minimizing subjectivity in weight assignment, improving resolution in thematic map reclassification, and securing adequate financial support to enhance the rigor and validity of flood susceptibility analysis.

6.6 Challenges and solutions

1. The response from local residents at the fringes of the ONP regarding previous flood events was unsatisfactory. This lack of information can hinder the understanding of historical flood patterns, which is crucial for effective

flood management and mitigation strategies. Several approaches can be taken to address this challenge. Working closely with local authorities, emergency management agencies and community leaders for long to access any existing data or documentation related to previous flood events can be helpful. Their expertise and knowledge of the area can enhance the understanding of historical flood patterns.

2. Obtaining cloud-free satellite data for the study area proved to be challenging, with only a 5% success rate despite multiple attempts. Cloud cover can obstruct visibility and hinder the interpretation of satellite imagery, impacting the accuracy of flood mapping and analysis. To address this challenge different satellite options with advanced imaging capabilities can be explored, such as high-resolution sensors or synthetic aperture radar technology, which are less affected by cloud cover. Historical weather patterns have to be identified to know about optimal time windows for data collection.

6.7 Recommendations

Effective flood management strategies for ONP (mainly in the high flood prone areas) are of utmost importance. Implementing a variety of strategies can mitigate the potential damage to the park's ecosystem and infrastructure.

1. Deployment of geobags along riverbanks: Geobags are large, durable bags filled with sand or soil used to reinforce and stabilize riverbanks. This strategy helps prevent erosion and protects against flooding by strengthening vulnerable areas along the riverbanks. It is a cost-effective and relatively simple solution that can be implemented quickly.
2. Reinforced concrete porcupines: Reinforced concrete porcupines are structures placed along riverbanks to slow down the flow of water and reduce erosion. These structures mimic natural features like rocks and logs, providing a habitat for aquatic species, while also serving a practical purpose in flood management. They are durable and low-maintenance, making them a sustainable option for long-term flood protection.
3. Levee construction: Levees are raised embankments built along rivers to contain floodwaters and prevent them from spilling over into surrounding areas. Constructing levees in high flood-prone areas of ONP can provide a reliable barrier against flooding, protecting both natural habitats and human settlements within the park.
4. Stone spurs: Stone spurs are structures built perpendicular to the riverbank to deflect water flow and reduce erosion. They are often made of large rocks or boulders arranged in a staggered pattern to create barriers that slow down the current. Stone spurs can be strategically placed in vulnerable areas to redirect water away from critical habitats and infrastructure.

5. Geomattresses and geotubes: Geomattresses and geotubes are flexible, erosion-control systems made from synthetic materials. They can be laid on the riverbed or installed along the banks to stabilize soil, prevent erosion, and protect against flooding. These innovative solutions offer versatility and adaptability, making them suitable for various terrain types within ONP.
6. Relocating animals from high-risk zones to safer areas within the park is a proactive measure that can help minimize the loss of wildlife during floods. By identifying and designating moderate and low-risk zones as relocation sites, park authorities can safeguard vulnerable species and reduce the overall impact of flooding on biodiversity. Additionally, the creation of flood diversion zones and storage areas for surplus water can help manage floodwaters more effectively, especially in regions with dense vegetation and sensitive ecosystems. These designated areas serve as buffers, absorbing excess water and reducing the risk of inundation in critical habitats.

6.8 Conclusion

One important area of research for a flood disaster study includes flood hazard mapping. It is important for effective emergency management planning and in making informed land use and protection decisions. In this study, the focus was on flood hazard mapping, a crucial aspect of disaster management, particularly in areas like the ONP. By utilizing the AHP model and considering nine significant flood-causing factors, we were able to construct a comprehensive flood hazard map using ArcGIS 10.8.2 software. This map categorized the park into four risk zones: low, moderate, high, and very high. The findings of our analysis indicate that a substantial portion of the ONP, approximately 35%, falls within the very high hazard risk zone, while an additional 39% is classified as high risk. Notably, the southern, south-eastern, and southwestern regions of the park emerged as particularly vulnerable to flooding, highlighting areas where focused mitigation efforts may be necessary. Furthermore, about 20% of the park's land area was identified as having a moderate hazard risk. ONP is not only a biodiversity hot-spot but also a habitat for numerous endangered species; effective flood management strategies are imperative. Our research contributes significantly by providing a detailed flood hazard map that can serve as a valuable resource for various stakeholders, including the Assam Disaster Management Authority, Brahmaputra Board, Assam Forest Department, hydrologists, engineers, environmentalists, and conservationists. By utilizing this map, decision-makers can make informed choices regarding land use, emergency response planning, and infrastructure development within the park. Additionally, it can aid in the formulation of targeted conservation efforts aimed at protecting the delicate ecosystem of ONP and mitigating the adverse impacts of flooding on both wildlife and human communities in the surrounding areas. Additionally, this study underscores the

importance of proactive flood management measures in safeguarding natural habitats and enhancing overall resilience to disasters. It highlights the critical role of interdisciplinary collaboration and data-driven approaches in addressing complex environmental challenges, ultimately contributing to the sustainable management of precious ecological resources like the ONP.

Acknowledgment

The authors are grateful to the faculty members of the Department of Geography, Cotton University, Guwahati, Assam for help and support.

References

- Ajin, R. S. (2013). Flood hazard assessment of Vamanapuram river basin, Kerala, India: An approach using remote sensing & GIS techniques. *Advances in Applied Science Research*, 4(3), 263–274.
- Ali, S. A., Khatun, R., Ahmad, A., & Ahmad, S. N. (2019). Application of GIS-based analytic hierarchy process and frequency ratio model to flood vulnerable mapping and risk area estimation at Sundarban region, India. *Modeling Earth Systems and Environment*, 5(3), 1083–1102. Available from <https://doi.org/10.1007/s40808-019-00593-z>, <http://springer.com/journal/40808>.
- Antoine, J., Fischer, G., & Makowski, M. (1997). Multiple criteria land use analysis. *Applied Mathematics and Computation*, 83(2–3), 195–215. Available from [https://doi.org/10.1016/S0096-3003\(96\)00190-7](https://doi.org/10.1016/S0096-3003(96)00190-7).
- Areendran, G., Raj, K., Sharma, A., Bora, P. J., Sarmah, A., Sahana, M., & Ranjan, K. (2020). Documenting the land use pattern in the corridor complexes of Kaziranga National Park using high resolution satellite imagery. *Trees, Forests and People*, 2, 100039. Available from <https://doi.org/10.1016/j.tfp.2020.100039>.
- Argaz, A. (2019). Flood hazard mapping using remote sensing and GIS Tools: A case study of souss watershed. *Journal of Materials and Environmental Sciences*, 10(2), 170–181.
- Armenakis, C., Du, E., Natesan, S., Persad, R., & Zhang, Y. (2017). Flood risk assessment in urban areas based on spatial analytics and social factors. *Geosciences*, 7(4), 123. Available from <https://doi.org/10.3390/geosciences7040123>.
- Arora, A., Pandey, M., Siddiqui, M. A., Hong, H., & Mishra, V. N. (2021). Spatial flood susceptibility prediction in Middle Ganga Plain: Comparison of frequency ratio and Shannon's entropy models. *Geocarto International*, 36(18), 2085–2116. Available from <https://doi.org/10.1080/10106049.2019.1687594>, <http://www.tandfonline.com/toc/tgei20/current>.
- Arya, A. K., & Singh, A. P. (2021). Multi criteria analysis for flood hazard mapping using GIS techniques: A case study of Ghaghara River basin in Uttar Pradesh, India. *Arabian Journal of Geosciences*, 14(8). Available from <https://doi.org/10.1007/s12517-021-06971-1>, http://www.springer.com/geosciences/journal/12517?cm_mmc=AD-_-enews-_-PSE1892-_-0.

- Bapalu, G. V., & Sinha, R. (2005). GIS in flood hazard mapping: A case study of Kosi River Basin, India. *GIS Development Weekly*, 1(13), 1–3. Available from <https://doi.org/10.13140/RG.2.1.1492.2720>.
- Bhatt, G. D., Sinha, K., Deka, P. K., & Kumar, A. (2014). Flood hazard and risk assessment in Chamoli District, Uttarakhand using satellite remote sensing and GIS techniques. *International Journal of Innovative Research in Science, Engineering and Technology*, 03(08), 15348–15356. Available from <https://doi.org/10.15680/IJRSET.2014.0308039>.
- Borah, J., Ahmed, M., & Sarma, P. (2010). Brahmaputra River islands as potential corridors for dispersing tigers: a case study from Assam, India. *International Journal of Biodiversity and Conservation*, 2, 350–358.
- Chakdar, B., Singha, H., & Choudhury, M. R. (2019). Bird community of Rajiv Gandhi Orang National Park, Assam. *Journal of Asia-Pacific Biodiversity*, 12(4), 498–507. Available from <https://doi.org/10.1016/j.japb.2019.07.003>, <http://www.journals.elsevier.com/journal-of-asia-pacific-biodiversity/>.
- Chakraborty, S., & Mukhopadhyay, S. (2019). Assessing flood risk using analytical hierarchy process (AHP) and geographical information system (GIS): Application in Coochbehar district of West Bengal, India. *Natural Hazards*, 99(1), 247–274. Available from <https://doi.org/10.1007/s11069-019-03737-7>, <http://www.wkap.nl/journalhome.htm/0921-030X>.
- Choudhury, A. U. (2000). *The birds of Assam*. Gibbon Books & WWF India NE Region.
- CRED. (2020). *EM-DAT, The Int disaster database*. Centre for Research on the Epidemiology of Disasters.
- Danumah, J. H., Odai, S. N., Saley, B. M., Szarzynski, J., Thiel, M., Kwaku, A., . . . Akpa, L. Y. (2016). Flood risk assessment and mapping in Abidjan district using multi-criteria analysis (AHP) model and geoinformation techniques, (cote d’ivoire). *Geoenvironmental Disasters*, 3(1). Available from <https://doi.org/10.1186/s40677-016-0044-y>, <https://link.springer.com/journal/40677>.
- Debbarma, A., & Deen, S. (2020). Flood disaster management in Assam. *Shodh Sanchar Bulletin*, 10(40), 105–109.
- Dhar, O. N., & Nandargi, S. (2004). Rainfall distribution over the Arunachal Pradesh Himalayas. *Weather*, 59(6), 155–157. Available from <https://doi.org/10.1256/wea.87.03>.
- Duan, W., He, B., Takara, K., Luo, P., Nover, D., Yamashiki, Y., & Huang, W. (2014). Anomalous atmospheric events leading to Kyushu’s flash floods, July 11–14, 2012. *Natural Hazards*, 73(3), 1255–1267. Available from <https://doi.org/10.1007/s11069-014-1134-3>, <http://www.wkap.nl/journalhome.htm/0921-030X>.
- El-Haddad, B. A., Youssef, A. M., Pourghasemi, H. R., Pradhan, B., El-Shater, A. H., & El-Khashab, M. H. (2021). Flood susceptibility prediction using four machine learning techniques and comparison of their performance at Wadi Qena Basin, Egypt. *Natural Hazards*, 105(1), 83–114. Available from <https://doi.org/10.1007/s11069-020-04296-y>, <http://www.wkap.nl/journalhome.htm/0921-030X>.
- Fernández, D. S., & Lutz, M. A. (2010). Urban flood hazard zoning in Tucumán Province, Argentina, using GIS and multicriteria decision analysis. *Engineering Geology*, 111 (1–4), 90–98. Available from <https://doi.org/10.1016/j.enggeo.2009.12.006>.
- Fonseca, A. R., Santos, M., & Santos, J. A. (2018). Hydrological and flood hazard assessment using a coupled modelling approach for a mountainous catchment in Portugal.

- Stochastic Environmental Research and Risk Assessment*, 32(7), 2165–2177. Available from <https://doi.org/10.1007/s00477-018-1525-1>, <http://link.springer-ny.com/link/service/journals/00477/index.htm>.
- Forkuo, E. K. (2011). Flood hazard mapping using Aster image data with GIS. *International Journal of Geomatics and Geosciences*, 4, 932–950.
- United Nations Office for Disaster Risk Reduction (UNDRR). (2017). *Gar Atlas: Unveiling global disaster risk*. UNDRR.
- Gil, Y., & Kellerman, A. (1993). A multicriteria model for the location of solid waste transfer stations: The case of Ashdod, Israel. *GeoJournal*, 29(4), 377–384. Available from <https://doi.org/10.1007/BF00807540>.
- Glas, H., Rocabado, I., Huysentruyt, S., Maroy, E., Salazar Cortez, D., Coorevits, K., ... Deruyter, G. (2019). Flood risk mapping worldwide: A flexible methodology and toolbox. *Water*, 11(11), 2371. Available from <https://doi.org/10.3390/w11112371>.
- Glenn, E. P., Morino, K., Nagler, P. L., Murray, R. S., Pearlstein, S., & Hultine, K. R. (2012). Roles of saltcedar (*Tamarix* spp.) and capillary rise in salinizing a non-flooding terrace on a flow-regulated desert river. *Journal of Arid Environments*, 79, 56–65. Available from <https://doi.org/10.1016/j.jaridenv.2011.11.025>.
- United Nations Office for Disaster Risk Reduction (UNDRR). (2019). *Global assessment report on disaster risk reduction*.
- Gupta, L., & Dixit, J. (2022). A GIS-based flood risk mapping of Assam, India, using the MCDA-AHP approach at the regional and administrative level. *Geocarto International*, 37(26), 11867–11899. Available from <https://doi.org/10.1080/10106049.2022.2060329>, <http://www.tandfonline.com/toc/tgei20/current>.
- Hallegatte, S., Green, C., Nicholls, R. J., & Corfee-Morlot, J. (2013). Future flood losses in major coastal cities. *Nature Climate Change*, 3(9), 802–806. Available from <https://doi.org/10.1038/nclimate1979>.
- Hammami, S., Zouhri, L., Souissi, D., Souei, A., Zghibi, A., Marzougui, A., & Dlala, M. (2019). Application of the GIS based multi-criteria decision analysis and analytical hierarchy process (AHP) in the flood susceptibility mapping (Tunisia). *Arabian Journal of Geosciences*, 12(21). Available from <https://doi.org/10.1007/s12517-019-4754-9>, http://www.springer.com/geosciences/journal/12517?cm_mmc=AD-_-enews-_-PSE1892-_-0.
- Hapuarachchi, H. A. P., Wang, Q. J., & Pagano, T. C. (2011). A review of advances in flash flood forecasting. *Hydrological Processes*, 25(18), 2771–2784. Available from <https://doi.org/10.1002/hyp.8040>.
- Hazarika, B. C., & Saikia, P. K. (2010). A study on the behaviour of Great Indian One-horned Rhino (*Rhinoceros unicornis* Linn.) in the Rajiv Gandhi Orang National Park. *NeBio*, 1(2), 62–74.
- Jhala, Y. V., & Qureshi, Q. (2019). *Status of tigers, co-predators and prey in India 2018. Summary report*. National Tiger Conservation Authority, Government of India.
- Khaing, Z. M., Zhang, K., Sawano, H., Shrestha, B. B., Sayama, T., Nakamura, K., & Schumann, G. J.-P. (2019). Flood hazard mapping and assessment in data-scarce Nyaungdon area, Myanmar. *PLoS One*, 14(11), e0224558. Available from <https://doi.org/10.1371/journal.pone.0224558>.
- Khosravi, K., Nohani, E., Maroufinia, E., & Pourghasemi, H. R. (2016). A GIS-based flood susceptibility assessment and its mapping in Iran: A comparison between frequency ratio and weights-of-evidence bivariate statistical models with multi-criteria

- decision-making technique. *Natural Hazards*, 83(2), 947–987. Available from <https://doi.org/10.1007/s11069-016-2357-2>, <http://www.wkap.nl/journalhome.htm/0921-030X>.
- Laouacheria, F., Kechida, S., & Chabi, M. (2019). Modelling the impact of design rainfall on the urban drainage system by storm water management model. *Journal of Water and Land Development*, 40(1), 119–125. Available from <https://doi.org/10.2478/jwld-2019-0013>, <http://versita.com/science/environment/jwld/>.
- Malczewski, J. (2000). On the use of weighted linear combination method in GIS: Common and best practice approaches. *Transactions in GIS*, 4(1), 5–22. Available from <https://doi.org/10.1111/1467-9671.00035>, [http://onlinelibrary.wiley.com/journal/10.1111/\(ISSN\)1467-9671](http://onlinelibrary.wiley.com/journal/10.1111/(ISSN)1467-9671).
- Muhadi, N. A., Abdullah, A. F., Bejo, S. K., Mahadi, M. R., & Mijic, A. (2020). The use of LiDAR-derived DEM in flood applications: A review. *Remote Sensing*, 12(14). Available from <https://doi.org/10.3390/rs12142308>, https://res.mdpi.com/d_attachment/remotesensing/remotesensing-12-02308/article_deploy/remotesensing-12-02308.pdf.
- Onușluel Gül, G. (2013). Estimating flood exposure potentials in Turkish catchments through index-based flood mapping. *Natural Hazards*, 69(1), 403–423. Available from <https://doi.org/10.1007/s11069-013-0717-8>, <http://www.wkap.nl/journalhome.htm/0921-030X>.
- Pai, D. S., Sridhar, L., Rajeevan, M., Sreejith, O. P., Satbhai, N. S., & Mukhopadhyay, B. (2014). Development of a new high spatial resolution ($0.25^\circ \times 0.25^\circ$) long period (1901-2010) daily gridded rainfall data set over India and its comparison with existing data sets over the region. *Mausam*, 65(1), 1–18. Available from http://www.imd.ernet.in/main_new.htm.
- Pohekar, S. D., & Ramachandran, M. (2004). Application of multi-criteria decision making to sustainable energy planning – A review. *Renewable and Sustainable Energy Reviews*, 8(4), 365–381. Available from <https://doi.org/10.1016/j.rser.2003.12.007>.
- Pourali, S. H., Arrowsmith, C., Chrisman, N., Matkan, A. A., & Mitchell, D. (2016). Topography wetness index application in flood-risk-based land use planning. *Applied Spatial Analysis and Policy*, 9(1), 39–54. Available from <https://doi.org/10.1007/s12061-014-9130-2>, <http://www.springer.com/geography/human+geography/journal/12061>.
- Rahmani, A. R., Narayan, G., Rosalind, L., & Sankaran R. (1990). Status of the Bengal Florican in India. In: *Status and ecology of the lesser and Bengal Floricans, with reports on Jerdon's courser and mountain quail. Final report* (pp. 55–78). Bombay Natural History Society.
- Rahmati, O., Falah, F., Naghibi, S. A., Biggs, T., Soltani, M., Deo, R. C., . . . Tien Bui, D. (2019). Land subsidence modelling using tree-based machine learning algorithms. *Science of the Total Environment*, 672, 239–252. Available from <https://doi.org/10.1016/j.scitotenv.2019.03.496>, <http://www.elsevier.com/locate/scitotenv>.
- Rahmati, O., Haghizadeh, A., & Stefanidis, S. (2016). Assessing the accuracy of GIS-based analytical hierarchy process for watershed prioritization; Gorganrood River Basin, Iran. *Water Resources Management*, 30(3), 1131–1150. Available from <https://doi.org/10.1007/s11269-015-1215-4>, <http://www.wkap.nl/journalhome.htm/0920-4741>.
- Rangari, V. A., Sridhar, V., Umamahesh, N. V., & Patel, A. K. (2019). Floodplain mapping and management of urban catchment using HEC-RAS: A case study of Hyderabad City. *Journal of The Institution of Engineers (India): Series A*, 100(1), 49–63.

- Available from <https://doi.org/10.1007/s40030-018-0345-0>, <http://www.springer.com/engineering/civil+engineering/journal/40030>.
- Rikalovic, A., Cosic, I., & Lazarevic, D. (2014). GIS based multi-criteria analysis for industrial site selection. *Procedia Engineering*, 69, 1054–1063. Available from <https://doi.org/10.1016/j.proeng.2014.03.090>, <http://www.sciencedirect.com/science/journal/18777058>.
- Rimba, A., Setiawati, M., Sambah, A., & Miura, F. (2017). Physical flood vulnerability mapping applying geospatial techniques in Okazaki City, Aichi Prefecture, Japan. *Urban Science*, 1(1), 7. Available from <https://doi.org/10.3390/urbansci1010007>.
- Saaty, T. L. (1977). A scaling method for priorities in hierarchical structures. *Journal of Mathematical Psychology*, 15(3), 234–281. Available from [https://doi.org/10.1016/0022-2496\(77\)90033-5](https://doi.org/10.1016/0022-2496(77)90033-5).
- Saaty, T. L. (1980). *The analytic hierarchy process*. Mc Graw Hill Company.
- Saaty, T. L. (1990). How to make a decision: The analytic hierarchy process. *European Journal of Operational Research*, 48(1), 9–26. Available from [https://doi.org/10.1016/0377-2217\(90\)90057-1](https://doi.org/10.1016/0377-2217(90)90057-1).
- Saaty, T. L. (2008). Decision making with the analytic hierarchy process. *International Journal of Services Sciences*, 1(1), 83. Available from <https://doi.org/10.1504/IJSSCI.2008.017590>.
- Saaty, T. L., & Vargas, L. G. (2000). *Models, methods, concepts and applications of the analytic hierarchy process*.
- Saki, F., Dehghani, H., Jodeiri Shokri, B., & Bogdanovic, D. (2020). Determination of the most appropriate tools of multi-criteria decision analysis for underground mining method selection—A case study. *Arabian Journal of Geosciences*, 13(23). Available from <https://doi.org/10.1007/s12517-020-06233-6>, http://www.springer.com/geosciences/journal/12517?cm_mmc=AD-_-enews-_-PSE1892-_-0.
- Saleh, S. K., Aliani, H., & Amoushahi, S. (2020). Application of modeling based on fuzzy logic with multi-criteria method in determining appropriate municipal landfill sites (case study: Kerman City). *Arabian Journal of Geosciences*, 13(22). Available from <https://doi.org/10.1007/s12517-020-06213-w>, http://www.springer.com/geosciences/journal/12517?cm_mmc=AD-_-enews-_-PSE1892-_-0.
- Samanta, R. K., Bhunia, G. S., Shit, P. K., & Pourghasemi, H. R. (2018). Flood susceptibility mapping using geospatial frequency ratio technique: A case study of Subarnarekha River Basin, India. *Modeling Earth Systems and Environment*, 4(1), 395–408. Available from <https://doi.org/10.1007/s40808-018-0427-z>, <http://springer.com/journal/40808>.
- Sandeep, B. V. (2020). *Tiger conservation plan 2021-30 Orang Tiger Reserve core area*. Assam Forest Department, GoI.
- Sarma, P. K., Mipun, B. S., Talukdar, B. K., Kumar, R., & Basumatary, A. K. (2011). Evaluation of habitat suitability for rhino (*Rhinoceros unicornis*) in Orang National Park using geo-spatial tools. *ISRN Ecology*, 2011, 1–9. Available from <https://doi.org/10.5402/2011/498258>.
- Shadmehri Toosi, A., Calbimonte, G. H., Nouri, H., & Alaghmand, S. (2019). River basin-scale flood hazard assessment using a modified multi-criteria decision analysis approach: A case study. *Journal of Hydrology*, 574, 660–671. Available from <https://doi.org/10.1016/j.jhydrol.2019.04.072>, <http://www.elsevier.com/inca/publications/store/5/0/3/3/4/3>.

- Shah, R. K., & Shah, R. K. (2023a). Forest cover change detection using remote sensing and GIS in Dibru-Saikhowa National Park, Assam: A spatio-temporal study. *Proceedings of the National Academy of Sciences India Section B: Biological Sciences*, 93(3), 559–564. Available from <https://www.springer.com/journal/40011>, <https://doi.org/10.1007/s40011-023-01449-4>.
- Shah, R. K., & Shah, R. K. (2023b). GIS-based flood susceptibility analysis using multi-parametric approach of analytical hierarchy process in Majuli Island, Assam, India. *Sustainable Water Resources Management*, 9(5). Available from <https://doi.org/10.1007/s40899-023-00924-0>, <https://www.springer.com/journal/40899>.
- Stefanidis, S., & Stathis, D. (2013). Assessment of flood hazard based on natural and anthropogenic factors using analytic hierarchy process (AHP). *Natural Hazards*, 68(2), 569–585. Available from <https://doi.org/10.1007/s11069-013-0639-5>.
- Subrahmanyam, V. P. (1988). Hazards of floods and droughts in India. In *Natural and man-made hazards. Proceedings of the symposium* (pp. 337–356). Rimouski, Quebec, 1986. Available from https://doi.org/10.1007/978-94-009-1433-9_24.
- Talukdar, B. N., & Sharma. (1995). *Checklist of the birds of Orang Wildlife Sanctuary*.
- Tsakiris, G. (2014). Flood risk assessment: Concepts, modelling, applications. *Natural Hazards and Earth System Sciences*, 14(5), 1361–1369. Available from <https://doi.org/10.5194/nhess-14-1361-2014>.
- Ullah, K., & Zhang, J. (2020). GIS-based flood hazard mapping using relative frequency ratio method: A case study of panjkora river basin, eastern Hindu Kush, Pakistan. *PLoS One*, 15(3). Available from <https://doi.org/10.1371/journal.pone.0229153>, <https://journals.plos.org/plosone/article/file?id=10.1371/journal.pone.0229153&type=printable>.
- Vojtek, M., & Vojteková, J. (2019). Flood susceptibility mapping on a national scale in Slovakia using the analytical hierarchy process. *Water*, 11(2), 364. Available from <https://doi.org/10.3390/w11020364>.
- Wang, J. J., Jing, Y. Y., Zhang, C. F., & Zhao, J. H. (2009). Review on multi-criteria decision analysis aid in sustainable energy decision-making. *Renewable and Sustainable Energy Reviews*, 13(9), 2263–2278. Available from <https://doi.org/10.1016/j.rser.2009.06.021>.
- Wang, Y., Li, Z., Tang, Z., & Zeng, G. (2011). A GIS-based spatial multi-criteria approach for flood risk assessment in the Dongting Lake Region, Hunan, Central China. *Water Resources Management*, 25(13), 3465–3484. Available from <https://doi.org/10.1007/s11269-011-9866-2>.
- Wiles, Jason J., & Levine, Norman S. (2002). A combined GIS and HEC model for the analysis of the effect of urbanization on flooding; The Swan Creek watershed, Ohio. *Environmental and Engineering Geoscience*, 8(1), 47–61. Available from <https://doi.org/10.2113/gsegeosci.8.1.47>.
- Youssef, A. M., Pradhan, B., & Sefry, S. A. (2016). Flash flood susceptibility assessment in Jeddah city (Kingdom of Saudi Arabia) using bivariate and multivariate statistical models. *Environmental Earth Sciences*, 75(1), 1–16. Available from <https://doi.org/10.1007/s12665-015-4830-8>, <http://www.springerlink.com/content/121380/>.
- Zhang, J., Zhou, C., Xu, K., & Watanabe, M. (2002). Flood disaster monitoring and evaluation in china. *Environmental Hazards*, 4(2), 33–43. Available from <https://doi.org/10.3763/ehaz.2002.0404>.

- Zhao, G., Xu, Z., Pang, B., Tu, T., Xu, L., & Du, L. (2019). An enhanced inundation method for urban flood hazard mapping at the large catchment scale. *Journal of Hydrology*, 571, 873–882. Available from <https://doi.org/10.1016/j.jhydrol.2019.02.008>, <http://www.elsevier.com/inca/publications/store/5/0/3/3/4/3>.
- Zwenzner, H., & Voigt, S. (2009). Improved estimation of flood parameters by combining space based SAR data with very high resolution digital elevation data. *Hydrology and Earth System Sciences*, 13(5), 567–576. Available from <https://doi.org/10.5194/hess-13-567-2009>, http://www.hydrol-earth-syst-sci.net/volumes_and_issues.html.